Mission Design for an Interstellar Probe with E-Sail Propulsion System

Mingying Huo

Department of Aerospace Engineering – Harbin Institute of Technology, 92 Xidazhi Street, Harbin 150001, China. E-mail: huomingying123@gmail.com

Giovanni Mengali

Department of Civil and Industrial Engineering – University of Pisa, 8 G. Caruso Street, Pisa I-56122, Italy. E-mail: g.mengali@ing.unipi.it

Alessandro A. Quarta *

Department of Civil and Industrial Engineering – University of Pisa, 8 G. Caruso Street, Pisa I-56122, Italy. E-mail: a.quarta@ing.unipi.it

---

Abstract

Missions towards the Solar System boundaries are of great scientific interest and represent a hard technological challenge. The use of an advanced propulsion system is a necessary means to maintain the flight time within reasonable limits. This paper analyzes missions to the heliosheath nose and to the heliopause nose, under the assumption that the primary propulsion system of the spacecraft is constituted by an electric solar wind sail. The study is performed using an optimal approach, by minimizing the total flight time required to reach a prescribed point of the Solar System. A number of results are presented using two mission parameters, i.e. the spacecraft maximum propulsive acceleration and the distance

at which the electric solar wind sail is jettisoned from the scientific probe. Numerical simulations show that an electric solar wind sail with performance consistent with the currently available technological level, is able to reach a solar distance of 100 au in about 23 years. The flight time can be further substantially reduced using an advanced electric solar wind sail with near-mid term technology.

Key words: Electric Solar Wind Sail, Heliopause and Heliosheath missions, Low-thrust optimal trajectories

---

Nomenclature

$\boldsymbol{a}_p$	=	propulsive acceleration vector
a_c	=	spacecraft characteristic acceleration
C	=	spacecraft center-of-mass
$\hat{\boldsymbol{i}}$, $\hat{\boldsymbol{j}}$, $\hat{\boldsymbol{k}}$	=	reference frame unit vectors
J	=	performance index
O	=	Sun's center-of-mass
$\boldsymbol{r}$	=	spacecraft position vector
t	=	time
$\boldsymbol{v}$	=	spacecraft velocity vector
α	=	cone angle
δ	=	clock angle
μ	=	gravitational parameter
τ	=	switching parameter

* Corresponding author.

Subscripts

f	=	final
max	=	maximum
O	=	orbital
$\oplus$	=	Earth
$\odot$	=	Sun

Superscripts

$\cdot$	=	time derivative
$\wedge$	=	unit vector

1 Introduction

A great interest exists in sending a spacecraft to the Solar System boundaries [1,2], to get information and solve fundamental scientific questions such as the nature of the nearby interstellar medium, the structure of the Sun-heliosphere system, the distribution of matter in this part of the interplanetary space, the way with which plasma, dust, particles and radiation interact in rarefied and not fully ionized plasmas. These and many other challenging questions can only be answered by means of missions that are capable of obtaining in situ measurements about the interstellar medium and the Sun's interactions with that medium. Fundamental information include, for example, the measurement of density, ionization state, dust composition and magnetic field strength as a function of the

Sun's distance.

Missions beyond the heliopause require the capability of reaching very long distances, about $100-200$ au, in a reasonable time interval and the space probe must be able to cruise at a speed on the order of 10 au/year or higher [3,4]. This is a rather demanding requirement, that implies the use of advanced propulsion systems. Apart from the chemical option, whose utility for these missions is limited by the sizeable propellant mass the spacecraft would require, a number of different thrusters have been proposed over the years for interstellar missions [5,6], including the use of solar and nuclear electric propulsion [7], laser beams [8], nuclear fusion [9,10], antimatter [11] and minimagnetospheric plasma propulsion [12]. Even though each of these systems has advantages and drawbacks, a key concept in such an advanced mission design is that of reliability. In fact, most of those propulsion systems lack of an adequate experimental application and the possibility of an use in future spacecraft mission is still questionable.

The most common choice and a promising option for an interstellar mission is probably related to the use of a (photonic) solar sail [13,14]. A number of studies exist, which confirm that the heliopause nose, at a distance of about 200 au, may be reached by a space probe propelled by a solar sail within a flight time of about 25 years [3,4]. Indeed, solar sails can provide a continuous thrust for the whole mission length and gain a large amount of ΔV in a reasonable time using a solar photonic assist maneuver [14,15,16]. A critical issue, in this regard, is that the close passage to the Sun (at about 0.14–0.25 au [17]) is a very challenging maneuver in terms of thermal load the probe must be able to bear.

In recent years the electric solar wind sail (E-sail) has appeared to be an interesting option for an interstellar mission. The E-sail is a new type of propellant-

less propulsion system, which uses the natural solar wind to produce propulsive thrust. A first example of scientific demonstration of the E-sail concept is being conducted by the ESTCube-1 satellite, whose main goal is to measure the strength of the "E-sail effect" in a low Earth orbit [18]. Another E-sail experiment is scheduled to be performed by Aalto-1 satellite, the first Finnish nanosatellite project, to be launched at the end of 2015.

The E-sail thrust concept has been used to calculate mission trajectories to the boundaries of the Solar System for realistic (scientific) payloads [19,20]. However, a detailed study regarding the feasibility of an interstellar mission with a refined thruster's mathematical model has not yet been performed. The aim of this paper is to provide new results and mission studies using an E-sail as a primary propulsion system and to improve in different ways the results from previous studies. The first improvement provided by this paper is in terms of mathematical model of the propulsion system. In previous papers [19,20] the propulsive thrust due to the E-sail was assumed to scale with the solar distance proportional to $(1/r)^{7/6}$, where r is the spacecraft distance from the Sun. However, more recent plasma dynamic simulations [21,22] have shown that the E-sail thrust per tether length is five times higher than what previously estimated and, more importantly, the thrust modulus scales proportional to $1/r$. Another difference is in terms of accuracy of the mathematical model adopted in the simulation. For example, the simulations of Ref. [19] were performed assuming a two-dimensional scenario without using a solar wind assist (SWA) maneuver to gain energy from a close approach with the Sun. A two dimensional scenario were also widely used in Ref. [20], even though a SWA maneuver was taken into account. The main improvements introduced in this paper can be summarized in these main points: 1) the spacecraft orbit is fully three-dimensional, including the Earth's

orbit which is modelled using an accurate JPL DE405/LE405 model [23]; 2) the propulsion system implements the more recent E-sail thrust model; 3) a detailed parametric analysis is given as a function of two performance parameters, one being the spacecraft characteristic acceleration, the other the distance at which the E-sail is jettisoned; 4) the mission analysis is performed using an optimal approach in which the minimization of the scalar performance index is obtained using a direct optimization approach combining a hybrid genetic algorithm and pseudospectral method. A constraint on the minimum allowable distance from the Sun is also implemented.

2 Mission analysis

Consider a spacecraft whose main propulsion system is constituted by an E-sail. With reference to Fig. 1, the spacecraft equations of motion in a heliocentric inertial frame $\mathcal{T}_{\odot}(O; x, y, z)$ of unit vectors $\hat{\boldsymbol{i}}$, $\hat{\boldsymbol{j}}$ and $\hat{\boldsymbol{k}}$, are:

$$\dot{\boldsymbol{r}} = \boldsymbol{v} \tag{1}$$

$$\dot{\boldsymbol{v}} = -\frac{\mu_{\odot}}{r^3}\,\boldsymbol{r} + \boldsymbol{a}_p \tag{2}$$

where $\boldsymbol{r}$ is the spacecraft position vector (with $r = \|\boldsymbol{r}\|$ is the Sun-spacecraft distance), $\boldsymbol{v}$ is the spacecraft inertial velocity vector, $\mu_{\odot}$ is the Sun's gravitational parameter and $\boldsymbol{a}_p$ is the propulsive acceleration vector. According to the recent plasma dynamic simulations by Janhunen [22], the propulsive acceleration vector can be written as

$$\boldsymbol{a}_p = a_c \left(\frac{r_{\oplus}}{r}\right) \hat{\boldsymbol{a}}_p \tag{3}$$

where a_c is the spacecraft characteristic acceleration (that is, the spacecraft maximum propulsive acceleration when the Sun-spacecraft distance is $r = r_{\oplus} \triangleq$

1 au), $\tau \in \{0, 1\}$ is the switching parameter ($\tau = 1$ if the propulsion system is on, $\tau = 0$ when it is switched off), which allows the presence of coasting arcs in the spacecraft trajectory to be modelled, and $\hat{\boldsymbol{a}}_p$ is the thrust unit vector. The components of $\hat{\boldsymbol{a}}_p$ can be conveniently written as a function of two control angles, α (cone angle) and $\delta \in [0, 2\pi]$ (clock angle) as follows:

$$\hat{\boldsymbol{a}}_p = \sin\alpha \, \cos\delta \, \hat{\boldsymbol{i}}_O + \sin\alpha \, \sin\delta \, \hat{\boldsymbol{j}}_O + \cos\alpha \, \hat{\boldsymbol{k}}_O \tag{4}$$

where $\hat{\boldsymbol{i}}_O$, $\hat{\boldsymbol{j}}_O$ and $\hat{\boldsymbol{k}}_O$ are the unit vectors of an orbital reference frame $\mathcal{T}_O(C;\, x_O, y_O, z_O)$ and are defined as (see also Fig. 1)

$$\hat{\boldsymbol{k}}_O \triangleq \boldsymbol{r}/r \qquad , \qquad \hat{\boldsymbol{j}}_O \triangleq \frac{\hat{\boldsymbol{k}} \times \hat{\boldsymbol{k}}_O}{\left\| \hat{\boldsymbol{k}} \times \hat{\boldsymbol{k}}_O \right\|} \qquad , \qquad \hat{\boldsymbol{i}}_O \triangleq \hat{\boldsymbol{j}}_O \times \hat{\boldsymbol{k}}_O \tag{5}$$

Note that the three unit vectors $\hat{\boldsymbol{i}}_O$, $\hat{\boldsymbol{k}}_O$ and $\hat{\boldsymbol{k}}$ are coplanar, whereas the angle between the direction of $\hat{\boldsymbol{i}}_O$ and the ecliptic plane is equal to $(\pi/2 - \phi)$ where ϕ is the ecliptic latitude of the spacecraft.

The two angles α and δ, together with the switching parameter τ, constitute the three control variables of the problem. In geometrical terms, the cone angle α is the angle between the direction of the position vector $\boldsymbol{r}$ (which is assumed to coincide with the propagation direction of the solar wind) and the thrust vector. The clock angle, instead, is the angle measured counterclockwise from the direction of $\hat{\boldsymbol{i}}_O$ to the projection of $\hat{\boldsymbol{a}}_p$ onto the plane $(x_O,\, y_O)$. Equation (4) is particularly useful as it emphasizes the dependence of the propulsive thrust on the cone angle α which, for stability reasons [24], is required to not exceed a maximum value of $\alpha_{\max} \simeq 35\,\text{deg}$. This amounts to imposing a constraint on the control variable in the form

$$\alpha \leq \alpha_{\max} \tag{6}$$

2.1 Mission phases

In this analysis, the spacecraft can be thought of being constituted by two main parts: an E-sail propulsion system with its support equipment, and a scientific probe that carries the payload. The mission starts at time $t_0 \triangleq 0$, when the spacecraft tracks the Earth's heliocentric orbit, see Fig. 2. Such an assumption is consistent with a spacecraft deployment on a parabolic (Earth) escape trajectory, i.e. with zero hyperbolic excess with respect to the starting planet. In the succeeding analysis, the Earth's orbital elements are taken from the JPL planetary ephemerides model DE405/LE405 [23].

The spacecraft is first accelerated by the propulsion system until it reaches a hyperbolic osculating orbit with a hyperbolic excess speed V_∞. The latter is necessary for the scientific probe to proceed in the outer Solar System region and its value must be sufficient to meet the mission requirements. During this propelled phase, the spacecraft tends to approach the Sun to boost the propulsion system effectiveness, by exploiting the increased available thrust due to the growing solar wind electron density and temperature. Such a SWA maneuver [20] must be carried out by enforcing that the spacecraft heliocentric distance does not fall below a prescribed minimum admissible value, $\min(r) \triangleq r_{\min} < 1\,\text{au}$, based on thermal and mechanical constraints involving the E-sail tethers. The value of $r_{\min}$ defines a forbidden spherical region, centered at the Sun, which the spacecraft must avoid, see Fig. 2. The mathematical constraint, to be met along the whole transfer, is therefore

$$r \geq r_{\min} \tag{7}$$

Preliminary estimates [25] suggest using $r_{\min} = 0.5\,\text{au}$ for aluminum tethers, whereas copper tethers are expected to guarantee a closer approach to the Sun,

that is, $r_{\min} = 0.33\,\text{au}$.

A minimum distance of 0.5 au is of course conservative, because the flight times required to reach a given target point tend to increase as $r_{\min}$ is increased. Note that when the value of $r_{\min}$ tends to 1 au, which roughly coincides with the Sun-spacecraft distance along the initial parking orbit, the optimal transfer trajectory turns into an increasing departure from the Sun, without the presence of any SWA maneuver. This kind of transfer trajectories are discussed in Ref. [19].

At time t_c, when the Sun-spacecraft distance is r_c and the spacecraft has a hyperbolic excess speed equal to V_∞, the E-sail propulsive system is jettisoned and the scientific probe continues its cruise phase according to a Keplerian motion, see Fig. 2. The value of V_∞ is an important mission parameter, which affects the mission performance. However, since a bijective relation exists between r_c and V_∞, it is convenient to fix the value of r_c (which is simpler to handle) being related to the Sun-spacecraft distance $r = \|\boldsymbol{r}\|$, see Eqs. (1)-(2). In this case, the value of V_∞ is an output of the trajectory optimization process.

The E-sail jettison is necessary for two reasons. Firstly, the propulsion system becomes ineffective as the distance from the Sun is sufficiently high, see Eq. (3). The second and more important reason is that the scientific instruments may better operate within a "clean" environment, that is, without any interference with the E-sail structure. For missions to the heliopause nose, the requirements are that the spacecraft at the final time t_f reaches a distance $r_f = 200\,\text{au}$ from the Sun, with an ecliptic longitude of $\psi_f = 254.5\,\text{deg}$ and a latitude of $\phi_f = 7.5\,\text{deg}$, respectively (see Fig. 1). In case of missions to the heliosheath nose, i.e. to the region just beyond the termination shock where interstellar gas and solar wind interact, the distance to be reached is about $r_f = 100\,\text{au}$, with the same

constraints on the final ecliptic longitude and latitude.

2.2 Trajectory design

Missions involving propellantless propulsion systems can be studied effectively by minimizing the total flight time t_f. The analysis of minimum-time trajectories, i.e. the analysis of optimal performance for a given mission scenario, has been addressed using a parametric approach, by varying the spacecraft characteristic acceleration a_c and the distance r_c at which the E-sail is jettisoned within suitable ranges. The differential system used in the simulation is constituted by the six scalar nonlinear equations obtained by projecting Eqs. (1)–(2) onto the inertial reference frame. For a given value of r_f and for each pair (a_c, r_c), the problem is to find the control variables $\tau(t)$, $\alpha(t)$ and $\delta(t)$ that minimize t_f while meeting the two constraints of Eqs. (6) and (7).

The optimization problem was solved using a hybrid genetic algorithm and a numerical method based on the Gauss pseudospectral approach described by Benson [26]. In particular, the continuous optimal control problem is transcribed into a discrete nonlinear programming problem by means of global polynomial approximations of the differential equations Eqs. (1)–(2). The transcribed problem is then solved by sequential quadratic programming, in which the initial state and control histories are obtained by a genetic algorithm. In this case, the genetic algorithm is used to conduct a random search within the space of feasible solutions and provide a reasonable initial guess for the state and control histories. In particular, the hybrid optimization method is able to look for the optimal solution without any external guess from the designer [27].

3 Numerical simulations

Taking into account the preliminary results discussed in Ref. [20], the range of spacecraft characteristic acceleration and jettison distance are assumed to be $a_c \in [1,\, 2]\,\mathrm{mm/s^2}$ and $r_c \in [10,\, 20]\,\mathrm{au}$, respectively. Indeed, small values of either a_c (less than $1\,\mathrm{mm/s^2}$) or r_c (less than $10\,\mathrm{au}$) would correspond to high values of flight times to the heliosheath, on the order of 25 years or higher. Moreover, the case $r_c > 20\,\mathrm{au}$ is of little importance as it would imply a late beginning of the scientific mission phase. Finally, an high value of a_c, greater than $2\,\mathrm{mm/s^2}$, is considered to be beyond the current technological capabilities.

3.1 Mission towards the heliosheath nose

The first mission case to be discussed involves the achievement of the heliosheath nose, at a distance $r_f = 100\,\mathrm{au}$ from the Sun and a position in the Solar System characterized by an ecliptic longitude $\psi_f = 254.5\,\mathrm{deg}$ and a latitude $\phi_f = 7.5\,\mathrm{deg}$, respectively. The constraint on the minimum distance is conservatively assumed to be $r_{\mathrm{min}} = 0.5\,\mathrm{au}$.

The parametric analysis of the optimal transfer enables a number of data to be obtained, which are collected, using contour curves, in Figs. 3–4. In particular, Fig. 3 shows that the optimal flight times have a marked dependence on the jettison distance and, even more, on the characteristic acceleration, especially for values of a_c around $1\,\mathrm{mm/s^2}$. The dependence of t_f on these two parameters is less pronounced for sufficiently high values of a_c. A good correlation exists between the simulation results of this paper and those previously discussed in [20], despite the different performance model of the propulsion system and the different

optimization technique used. Figure 3 shows that flight times less than 25 years can be obtained with characteristic accelerations on the order of 1 mm/s^2, thus confirming the interesting potentialities of an E-sail-based propulsion system. To give a comparison term, the interstellar probe Voyager 1, launched on September 1977, reached the heliosheath on May 2005, i.e. after a 28 years flight.

Figure 4 shows the hyperbolic excess speed V_∞ achieved by the spacecraft at the end of the propelled phase. Note that the obtainable values of V_∞ are strongly dependent on the pair (a_c, r_c). The hyperbolic excess speed is a fundamental parameter for this kind of missions as it allows the spacecraft performance to be estimated during the coasting phase of the mission. As a matter of fact, if V_c is the modulus of the spacecraft velocity when the E-sail is jettisoned (that is, at time t_c), Fig. 5 shows that the ratio V_∞/V_c is near unity especially for medium-high values of a_c and jettison distances greater than about 12 au. Clearly, when V_∞/V_c approaches one, the spacecraft is close to the so called cruise condition (a condition that is reached in the proximity of the asymptote of the hyperbolic orbit after the E-sail jettison). When $t > t_c$, the spacecraft heliocentric trajectory can be approximated as a straight line that the spacecraft tracks at a nearly constant velocity. The time required to reach a given distance from the Sun (greater than r_c) is therefore easily estimated from

$$t \simeq t_c + \frac{r - r_c}{V_\infty} \tag{8}$$

where V_∞ depends on r_c (and a_c) according to the results shown in Fig. 5.

Having found the spacecraft performance in the conservative case of $r_{\min} = 0.5$ au, a sensitivity study of the results has been performed by varying the minimum distance from the Sun in the set $r_{\min} \in \{0.33, 0.4, 0.5\}$ and assuming a conservative value $r_c = 10$ au for the E-sail jettison distance. The simulation

results are illustrated in Figs. 6–7. In particular, Fig. 6 shows that the flight time t_f, a_c and r_c being equal, is quite sensitive to the constraint on $r_{\min}$. For example, when the minimum distance is reduced from 0.5 au to 0.33 au, the flight time decreases as much as $25-30\%$ depending on the value of the characteristic acceleration within its variation range.

Likewise, there is a significant variation of V_∞, which increases as long as $r_{\min}$ decreases, as is shown in Fig. 7. Assuming, for example, a characteristic acceleration of $1\,\mathrm{mm/s^2}$, if $r_{\min}$ is reduced to 0.33 au, the heliosheath can be reached in about 17 years, with a hyperbolic excess speed greater than 5.5 au/year. This means that the heliopause could be reached by adding 18 years of flight, with a total flight time of about 35 years.

3.2 Mission towards the heliopause nose

The optimization of a mission to the heliopause nose requires a minimization of t_f with a constraint on the final distance of $r_f = 200$ au. In this case the optimization procedure provides the results summarized in Fig. 8 where a conservative value of $r_{\min} = 0.5$ au is assumed. The figure shows that the required distance may be reached in about 47 years using a characteristic acceleration of $1\,\mathrm{mm/s^2}$ and an E-sail jettison distance of 10 au. The flight times can be approximately halved by doubling the jettison distance. Of course, the same flight time can also be obtained with smaller values of r_c, but either increasing the characteristic acceleration value, or decreasing $r_{\min}$.

For example, an advanced performance E-sail, with $a_c = 2\,\mathrm{mm/s^2}$, could theoretically reach the heliopause nose in about 24 years, assuming a jettison distance of

10 au. The corresponding flight trajectory, during the propelled phase, is shown in Fig. 9.

In a first phase the spacecraft is driven below the Earth's orbital plane. Then it moves to the Sun to perform a SWA maneuver at a distance equal to $r_{\min}$ (in this case 0.5 au) and eventually reaches the E-sail jettison distance after 817 days (2.2 years).

4 Conclusions

Missions beyond the boundaries of the Solar System have been discussed for a spacecraft whose primary propulsion system is an electric solar wind sail, which exploits the solar wind dynamic pressure for generating a continuous thrust without the need for reaction mass. Two different cases have been discussed, according to whether the final distance to reach is 100 au or 200 au. The two mission types have been studied using an optimal approach, by minimizing the flight time to reach the prescribed distance. The optimal trajectory is fully three-dimensional and includes a solar wind assist phase to gain energy from a close approach with the Sun. The primary propulsion system is then jettisoned when the spacecraft reaches a suitable solar distance and, after that, the probe continues its mission with a flight by inertia.

A parametric analysis of the problem has been performed, by varying the spacecraft characteristic acceleration, the propulsion system jettison distance and the distance at which the solar wind assist maneuver takes place. An electric solar wind sail with currently available technology is estimated to reach a distance of 100 au in about 23 years and a distance of 200 au in about 46 years. These

values can be however sensibly reduced with an advance of electric solar wind sail technology. For example, using a characteristic acceleration of $2\,\mathrm{mm/s^2}$, the previous distances could be reached in a time range that is less than halved. These results confirm that an electric solar wind sail represents an interesting option for an interstellar space mission.

5 Acknowledgments

The first author wish to thank the Shanghai Aerospace Science and Technology Foundation of China (Grant no. SAST201312).

References

[1] I. A. Crawford. "Avoiding intellectual stagnation: The starship as an expander of minds". *Journal of the British Interplanetary Society*, 67 253–257, 2014.

[2] M. A. G. Michaud. "Long-term perspectives on interstellar flight". *Journal of the British Interplanetary Society*, 67 207–212, 2014.

[3] P. Falkner, M. L. van de Berg, D. Renton, A. Atzei, A. Lyngvi and A. Peacock. "Update on ESA's technology reference studies". 56th International Astronautical Congress, Fukuoka, Japan, 2005. Paper IAC-05-A3.2A.07.

[4] A. E. Lyngvi, M. L. van den Berg and P. Falkner. "Study overview of the interstellar heliopause probe". Technical Report 3 (revision 4), ESA, 2007.

[5] G. L. Matloff. "The speed limit for graphene interstellar solar photon sails". *Journal of the British Interplanetary Society*, 66 377–380, 2013.

[6] G. L. Matloff. "Graphene solar photon sails and interstellar arks". *Journal of the British Interplanetary Society*, 67 237–248, 2014.

[7] R. McNutt, G. Andrews, J. McAdams, R. Gold, A. Santo, D. Oursler, K. Heeres, M. Fraeman and B. Williams. "Low-cost interstellar probe". *Acta Astronautica*, 52 267–279, 2003. doi:10.1016/S0094-5765(02)00166-2.

[8] R. L. Forward. "Roundtrip interstellar travel using laser-pushed lightsails". *Journal of Spacecraft and Rockets*, 21 187–195, 1984. doi:10.2514/3.8632.

[9] T. Kammash. "Pulsed fusion propulsion system for rapid interstellar missions". *Journal of Propulsion and Power*, 16 1100–1104, 2000. doi:10.2514/2.5683.

[10] J. French. "Project Icarus: A review of the Daedalus main propulsion system". *Journal of the British Interplanetary Society*, 66 248–251, 2013.

[11] R. L. Forward. "Antiproton annihilation propulsion". *Journal of Propulsion and Power*, 1 370–374, 1985. doi:10.2514/3.22811.

[12] R. M. Winglee, P. Euripides, T. Ziemba, J. Slough and L. Giersch. "Simulation of mini-magnetospheric plasma propulsion (M2P2) interacting with an external plasma wind". In "39th Joint Propulsion Conference and Exhibition", AIAA Paper 2003-5225, Huntsville, 2003.

[13] C. G. Sauer, Jr. "Solar sail trajectories for solar polar and interstellar probe missions". In "AAS/AIAA Astrodynamics Specialist Conference", AAS Paper 99-336, 1999.

[14] B. Dachwald. "Optimal solar sail trajectories for missions to the outer solar system". *Journal of Guidance, Control, and Dynamics*, 28 1187–1193, 2005. doi: 10.2514/1.13301.

[15] B. Dachwald. "Solar sail performance requirements for missions to the outer solar system and beyond". In "55^{th} International Astronautical Congress", Paper IAC–04–S.P.11, Vancouver, Canada, 2004.

[16] M. Leipold and O. Wagner. "Solar photonic assist' trajectory design for solar sail missions to the outer solar system and beyond". In T. H. Stengle, editor, "Advances in Astronautical Sciences", AAS/GSFC International Symposium on Space Flight Dynamics, Greenbelt, Maryland, 1998, volume Volume 100, Part 1. Paper AAS 98-386.

[17] V. Lappas, M. Leipold, A. Lyngvi, P. Falkner, H. Fichtner and S. Kraft. "Interstellar heliopause probe: System design of a solar sail mission to 200 au". In "AIAA Guidance, Navigation, and Control Conference and Exhibit", AIAA Paper 2005–6084, San Francisco, CA, 2005.

[18] J. Envall et al. "E-sail test payload of the ESTCube-1 nanosatellite". *Proceedings of the Estonian Academy of Sciences*, 63 210–221, 2014.

[19] G. Mengali, A. A. Quarta and P. Janhunen. "Considerations of electric sailcraft trajectory design". *Journal of the British Interplanetary Society*, 61 326–329, 2008.

[20] A. A. Quarta and G. Mengali. "Electric sail mission analysis for outer solar system exploration". *Journal of Guidance, Control, and Dynamics*, 33 740–755, 2010. doi: 10.2514/1.47006.

[21] P. Janhunen. "Increased electric sail thrust through removal of trapped shielding electrons by orbit chaotisation due to spacecraft body". *Annales Geophysicae*, 27 3089–3100, 2009. doi:10.5194/angeo-27-3089-2009.

[22] P. Janhunen. "The electric solar wind sail status report". In "European Planetary Science Congress 2010", Rome, Italy, 2010, volume 5. Paper EPSC 2010-297.

[23] E. M. Standish. "JPL planetary and lunar ephemerides, DE405/LE405". Interoffice Memoradum IOM 312.F-98-048, Jet Propulsion Laboratory, 1998.

[24] G. Mengali, A. A. Quarta and P. Janhunen. "Electric sail performance analysis". *Journal of Spacecraft and Rockets*, 45 122–129, 2008. doi:10.2514/1.31769.

[25] P. Janhunen et al. "Electric solar wind sail: Toward test missions". *Review of Scientific Instruments*, 81 111301.1–111301.11, 2010. doi:10.1063/1.3514548.

[26] D. Benson. *A Gauss Pseudospectral Transcription for Optimal Control*. Ph.D. Thesis, Massachusetts Institute of Technology, 2005. Retrievable at http://hdl.handle.net/1721.1/28919.

[27] N. Qi, M. Huo and Q. Yuan. "Displaced electric sail orbits design and transition trajectory optimization". *Mathematical Problems in Engineering*, 2014 1–9, 2014. doi:10.1155/2014/932190.

List of Figures

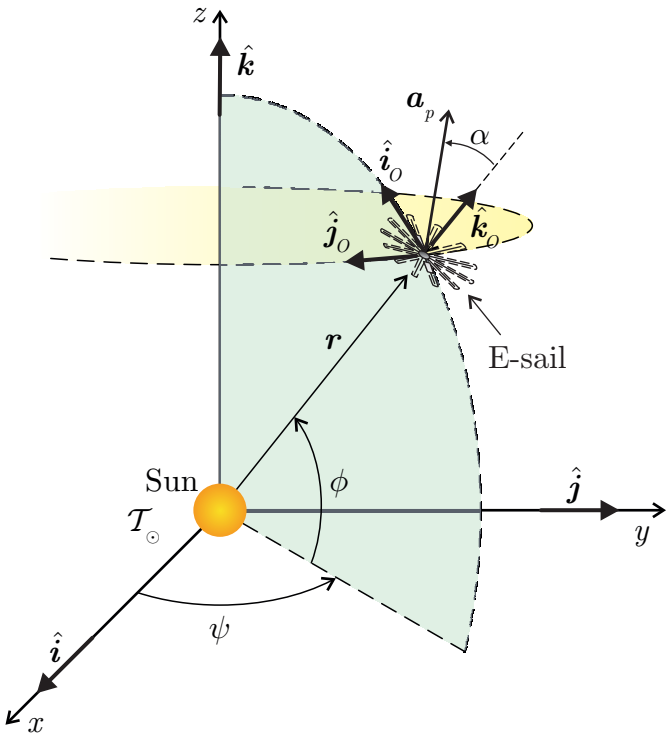

Figure 1. Reference frame and characteristic angles.

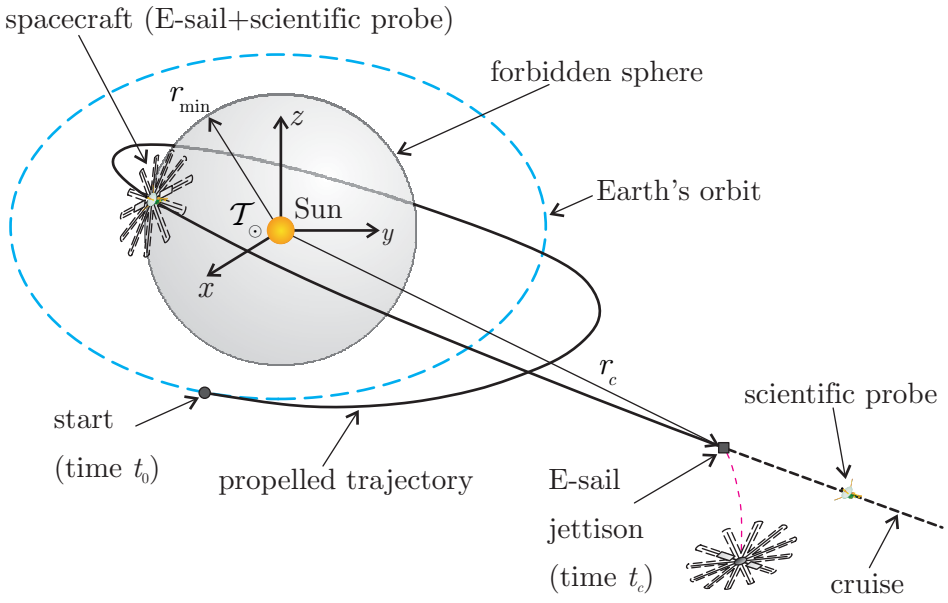

Figure 2. Schematic view of the mission phases.

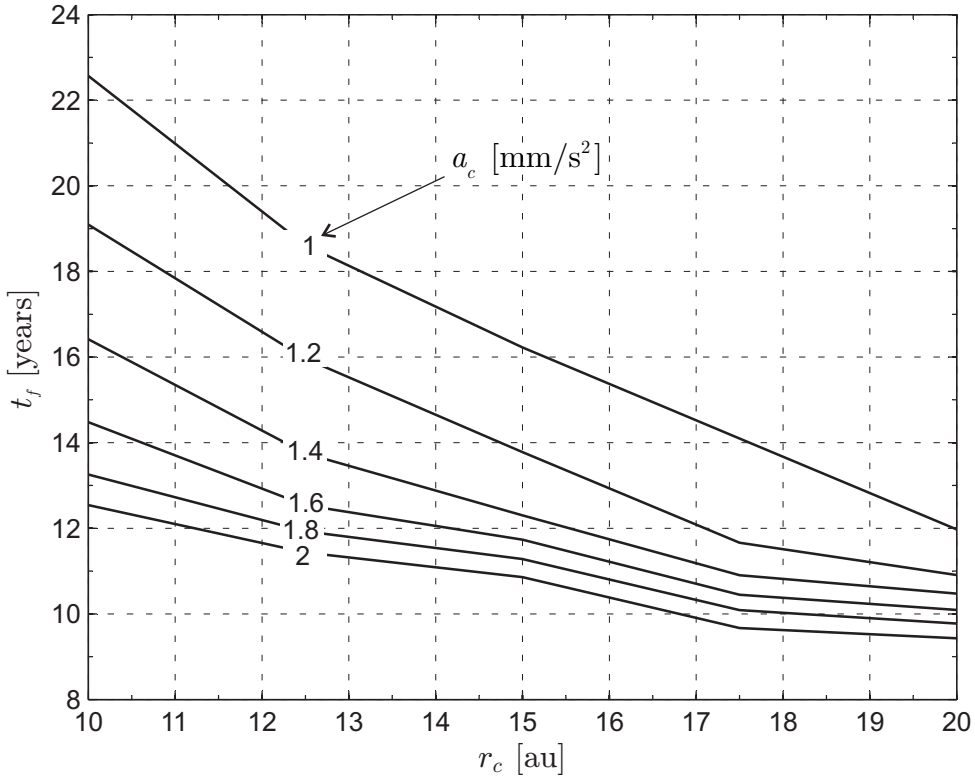

Figure 3. Minimum flight times for a mission towards the heliosheath, as a function of a_c and r_c ($r_{\min} = 0.5\,\mathrm{au}$).

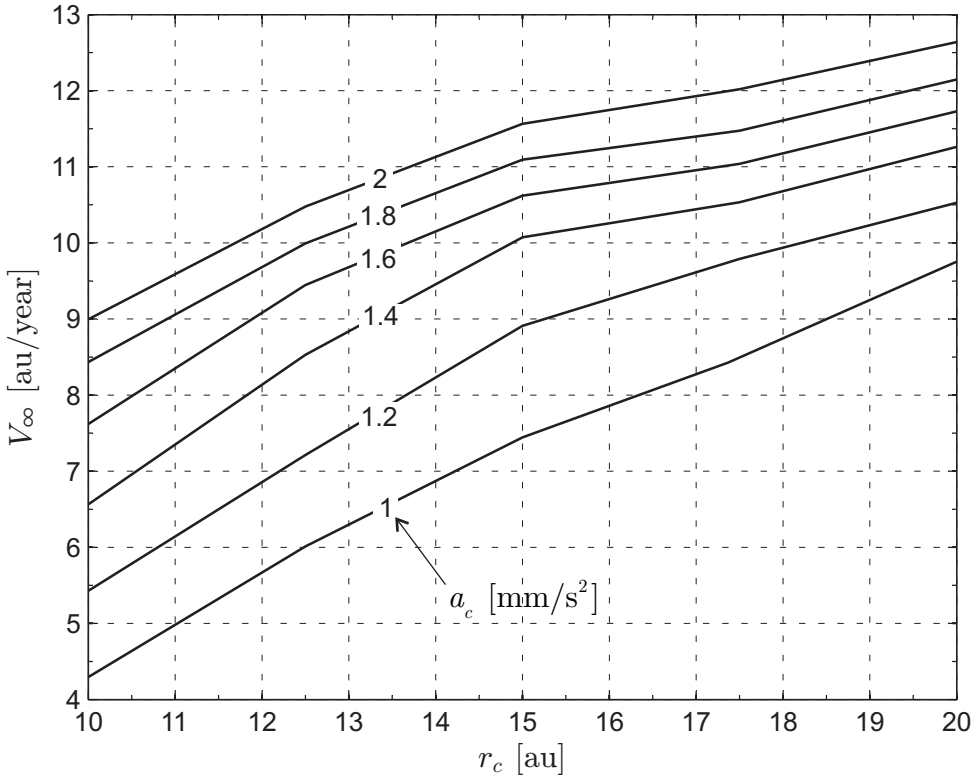

Figure 4. Hyperbolic excess speed for a mission towards the heliosheath, as a function of a_c and r_c ($r_{\min} = 0.5\,\mathrm{au}$).

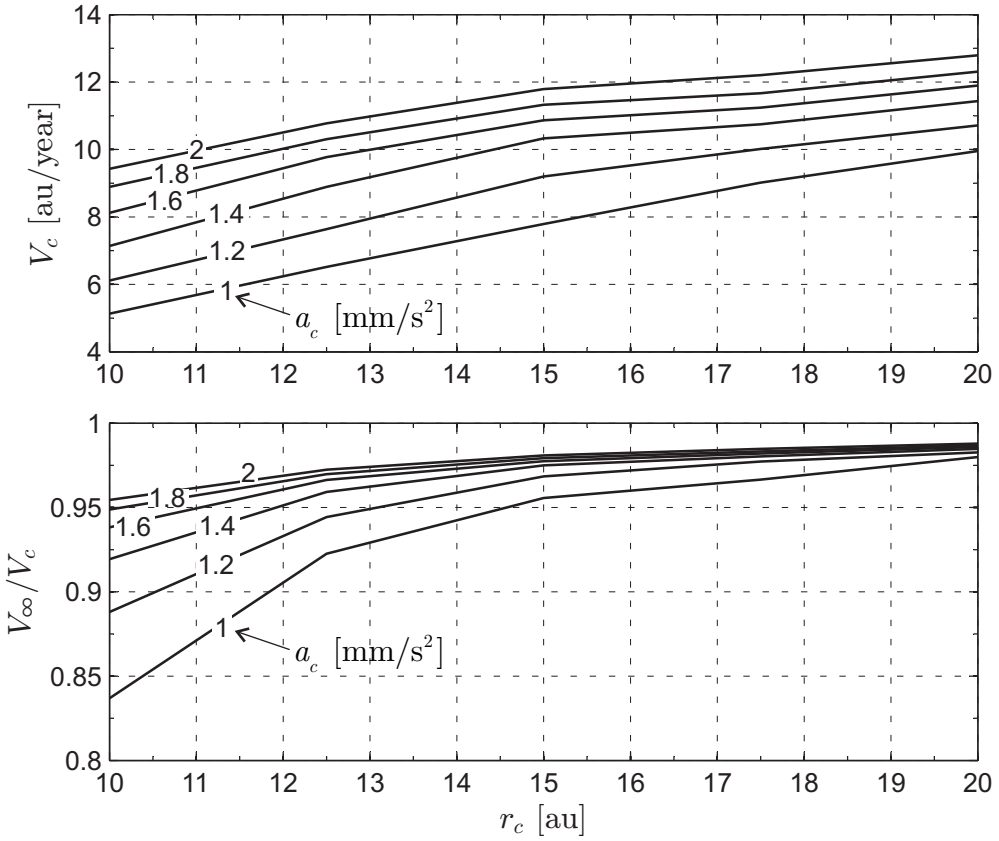

Figure 5. Cut-off speed for a mission towards the heliosheath, as a function of a_c and r_c ($r_{\min} = 0.5\,\mathrm{au}$).

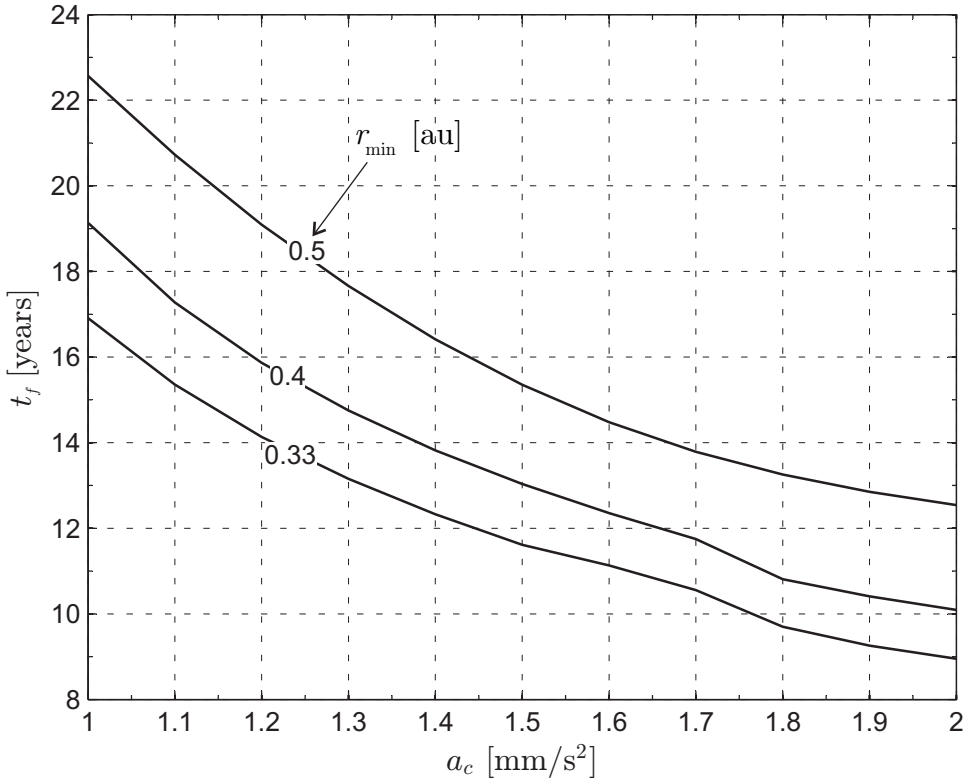

Figure 6. Minimum flight times for a mission towards the heliosheath, as a function of a_c and $r_{\min}$ ($r_c = 10\,\text{au}$).

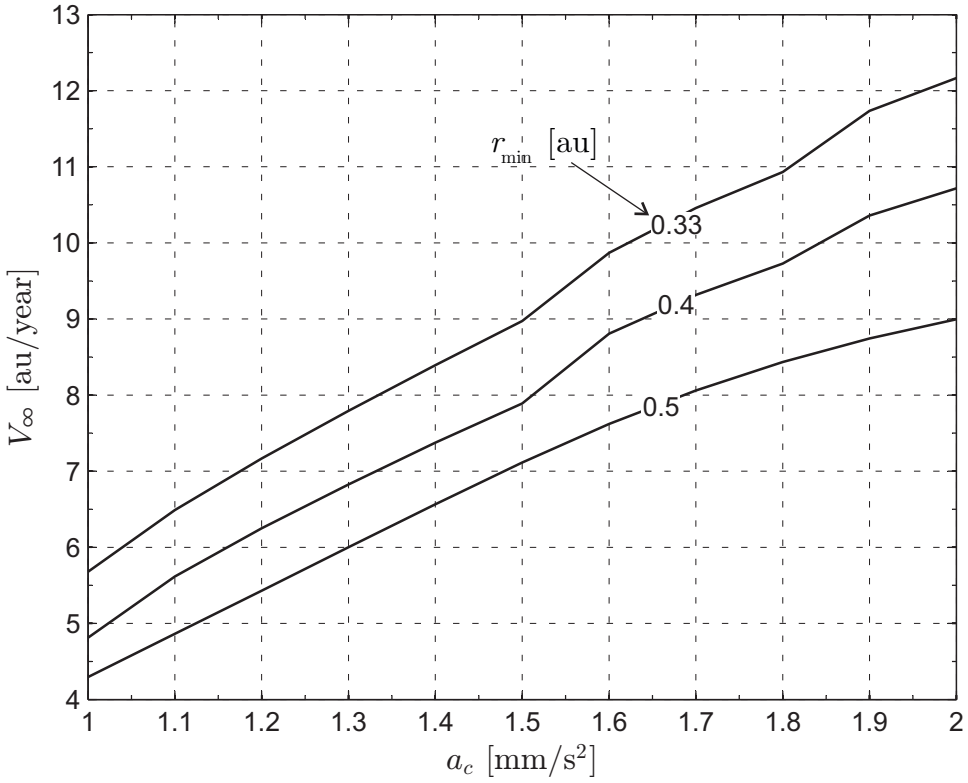

Figure 7. Hyperbolic excess speed for a mission towards the heliosheath, as a function of a_c and $r_{\min}$ ($r_c = 10\,\text{au}$).

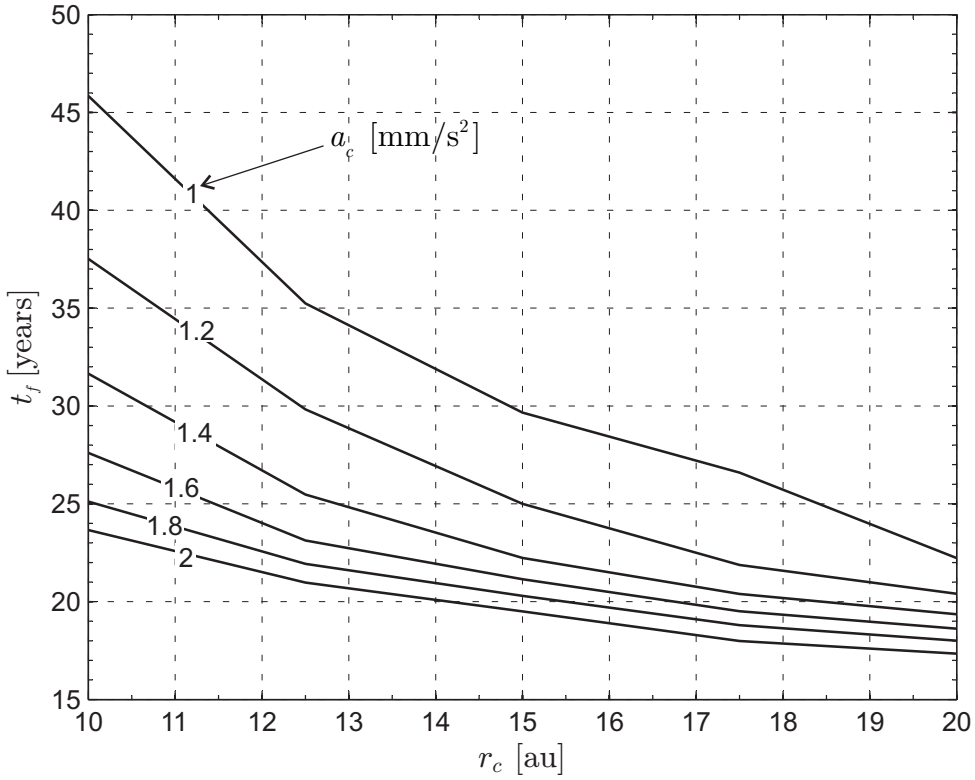

Figure 8. Minimum flight times for a mission towards the heliopause nose, as a function of a_c and r_c ($r_{\min} = 0.5\,\text{au}$).

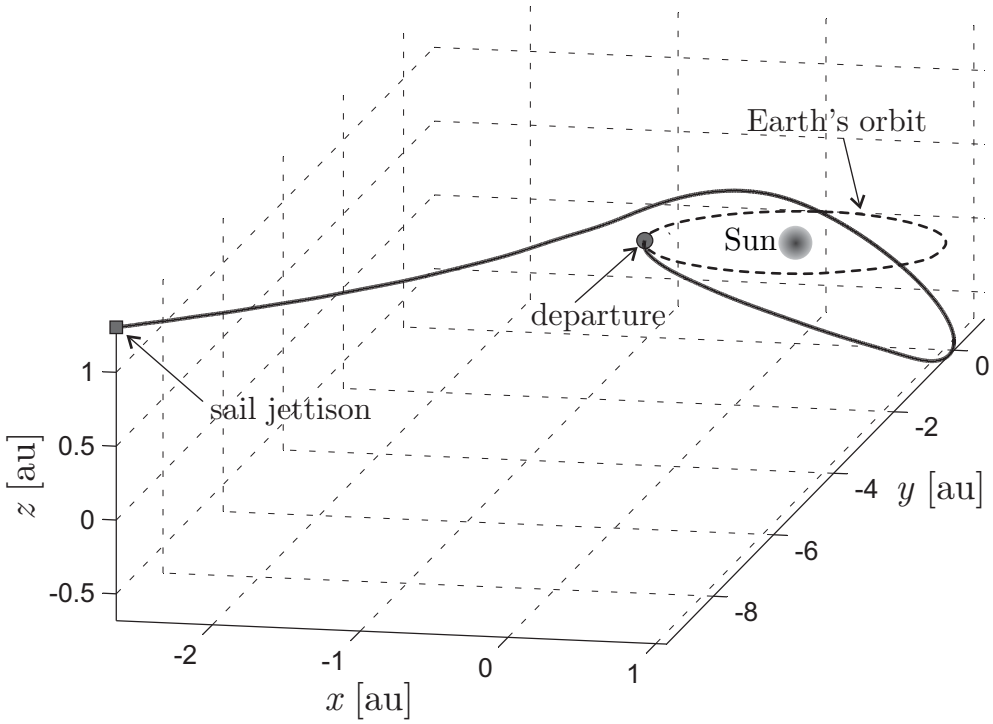

Figure 9. First part of the optimal trajectory towards the heliopause nose, with $a_c = 2$ mm/s^2, $r_{\min} = 0.5$ au and $r_c = 10$ au.